Analysis of Mixtures of Ferrocyanide and Ferricyanide using UV-Visible Spectroscopy for Characterisation of a Novel Redox Flow Battery

[1]MOHAMMED HARUN CHAKRABARTI* AND [2]EDWARD PELHAN LINDFIELD ROBERTS
[1]*Department of Environmental Engineering, NED University of Engineering and Technology, Karachi, Pakistan.*
[2]*School of Chemical Engineering and Analytical Sciences, University of Manchester, UK.*

(Received 2nd November 2007, revised 7th July 2008)

Summary: A novel Redox Flow Battery (RFB) was designed and developed at the University of Manchester. This system eliminated the ion-exchange membrane altogether by employing porous flow through electrodes. This system was characterised [1] using the ferrocyanide/ferricyanide [hexacyanoferrate (II)/hexacyanoferrate (III)] redox couple which had relatively fast electrochemical kinetics at several electrode surfaces. In this study an accurate method had been developed to determine the concentrations of the ferrocyanide/ferricyanide species from samples obtained from the battery. UV/Visible spectroscopy was chosen as the analytical tool for this purpose. Analysis of a range of standard solutions showed that by measuring the absorbance 260 nm and 420 nm it was possible to determine the concentration of both ferrocyanide and ferricyanide ions in a mixture of the two active species. Using the correlations developed, it was possible to determine the concentrations of ferrocyanide and ferricyanide ions to an accuracy of ± 4% in mixtures with concentrations in the range 0.01 to 0.1 mM. In work reported elsewhere [1] this analytical method was used to characterise the Redox Flow Battery and it was found that high conversion (>90%) could be achieved at relatively high concentrations (0.1 M) of the active species.

Introduction

Under growing pressure from high oil prices, the governments in developing countries are encouraging research in renewable energy technologies. Among them, the most notable are solar, wind, geothermal, tidal, biogas, biodiesel and others. Pakistan being located in a very hot and sunny region of the world can capitalize mainly from solar energy.

Several technologies have emerged over the years for the efficient storage of solar energy. These include flywheel energy storage, hydrogen based storage, capacitors, electrochemical and others [2]. The electrochemical technology has been used successfully for energy storage for a long time and various different systems have been researched upon [3, 4]. One possible system with a huge potential for efficient storage of solar energy is the Redox Flow Battery [5]. As opposed to conventional lead-acid type batteries, negative and positive electrolytes in the Redox Flow Battery are pumped from storage tanks or reservoirs to a cell composed of electrodes separated by an ion exchange membrane [5]. The redox reactions occur at electrodes during charging and discharging, converting electrical energy into chemical energy and *vice versa*.

Several different types of electrolytes have been tested in the past [5] but problems of electrolyte cross-contamination and high costs of ion exchange separators have always plagued the system. One possible solution to the problem of cross contamination was the use of a single species with different oxidation states as active electrolytes. This was how the concept of an all-vanadium Redox Flow Battery was born [6]. This system, since its conception in 1985, has already been commercialized due to its high charge/discharge efficiency [7]. However, problems still remain due to high costs and technical issues associated with the ion exchange membrane [8]. This problem has been addressed in new research endeavours conducted at the University of Manchester for several years [1, 9-11]. A novel Redox Flow Battery system was developed that eliminated the ion exchange separator altogether in response to the general problems being faced by the redox flow battery technology. Its electrochemical characteristics needed to be ascertained, however and this research work was conducted as a result.

In general, electrochemical cells have been characterised in various research works using the reversible ferrocyanide/ferricyanide redox couple [12,

*To whom all correspondence should be addressed.

13]. Concentrations of the ferrocyanide and ferricyanide ions in solution were determined using UV-Visible spectroscopy in most cases [14-16]. UV-Vis spectroscopy has had applications in various other research areas as well [17-20] and was considered as an ideal analytical tool for the characterisation of the novel Redox Flow Battery employed in this work.

Results and Discussion

The results were obtained for standard samples of potassium ferrocyanide [$K_4Fe(CN)_6$] and potassium ferricyanide [$K_3Fe(CN)_6$] at a range of concentrations as shown in Tables 1 and 2. Fig. 1 shows the absorption spectra for 0.025 mM $K_4Fe(CN)_6$ and a range of concentrations of $K_3Fe(CN)_6$. Fig. 2 shows the absorption spectra for 0.050 mM $K_4Fe(CN)_6$ and a range of concentrations of $K_3Fe(CN)_6$. Fig. 3 shows the absorption spectra for 0.075 mM $K_4Fe(CN)_6$ and a range of concentrations of $K_3Fe(CN)_6$. Fig. 4 shows the absorption spectra for 0.100 mM $K_4Fe(CN)_6$ and a range of concentrations of $K_3Fe(CN)_6$. These figures suggest that when the concentration of $K_4Fe(CN)_6$ was fixed while that of $K_3Fe(CN)_6$ was increased, a linear increase in the absorbance with concentration of $K_3Fe(CN)_6$ occurred at wavelengths, λ = 420, 317, 303 and 260 nm, as expected from the Beer-Lambert law. For these purposes of work, it was decided to investigate the effect of concentration on UV/Vis absorbance at wavelengths of 420 and 260 nm (at 420 nm, absorbance was more towards the visible range of the electromagnetic spectrum whereas at 260 nm, absorbance was in the UV range). Fig. 5 shows the relationship between absorbance at 260 nm and standard concentrations of $K_4Fe(CN)_6$ for a range of concentrations of $K_3Fe(CN)_6$. Similarly Fig. 6 shows the relationship between absorbance at 420 nm and standard concentrations of $K_4Fe(CN)_6$ for a range of concentrations of $K_3Fe(CN)_6$. Both Fig. 5 and Fig. 6 show a linear relationship between absorbance at 260 and 420 nm and concentrations of $K_3Fe(CN)_6$ thus confirming the original observations from Figs. 1-4.

Fig. 7 shows the absorption spectra for 0.025 mM $K_3Fe(CN)_6$ and a range of concentrations of $K_4Fe(CN)_6$. Fig. 8 shows the absorption spectra for 0.050 mM $K_3Fe(CN)_6$ and a range of concentrations of $K_4Fe(CN)_6$. Fig. 9 shows the absorption spectra for 0.075 mM $K_3Fe(CN)_6$ and a range of concentrations of $K_4Fe(CN)_6$. Fig. 10 shows the absorption spectra for 0.100 mM $K_3Fe(CN)_6$ and a range of concentrations of $K_4Fe(CN)_6$. As can be seen from these figures, when the concentration of

Table-1: Composition of standard samples for characterising the absorbance of UV and visible light against the concentrations of $Fe(CN)_6^{3-}$ ions.

Concentration of $K_4Fe(CN)_6$ (mM)	Concentration of $K_3Fe(CN)_6$ (mM)
0.025	0
	0.01
	0.025
	0.05
	0.075
	0.1
0.05	0
	0.01
	0.025
	0.05
	0.075
	0.1
0.075	0
	0.01
	0.025
	0.05
	0.075
	0.1
0.1	0
	0.01
	0.025
	0.05
	0.075
	0.1

Table-2: Composition of standard samples for characterising the absorbance of UV and visible light against the concentrations of $Fe(CN)_6^{2-}$ ions.

Concentration of $K_4Fe(CN)_6$ (mM)	Concentration of $K_3Fe(CN)_6$ (mM)
0	0.025
0.01	
0.025	
0.05	
0.075	
0.1	
0	0.05
0.01	
0.025	
0.05	
0.075	
0.1	
0	0.075
0.01	
0.025	
0.05	
0.075	
0.1	
0	0.1
0.01	
0.025	
0.05	
0.075	
0.1	

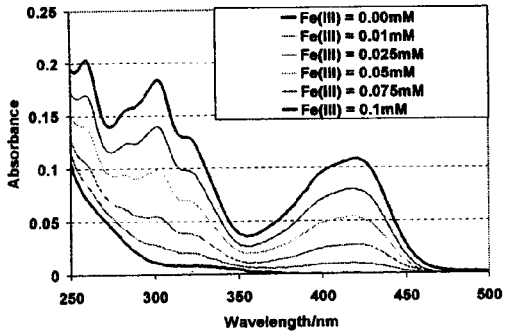

Fig. 1: UV Spectra for 0.025 mM $K_4Fe(CN)_6$ and a range of concentrations of $K_3Fe(CN)_6$ [denoted as Fe(III) in the legend above] in 0.25 mM K_2CO_3 solutions.

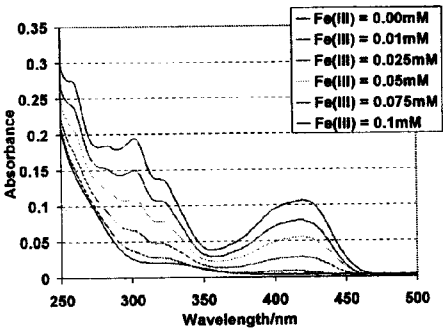

Fig. 2: UV Spectra for 0.050 mM $K_4Fe(CN)_6$ and a range of concentrations of $K_3Fe(CN)_6$ [denoted as Fe(III) in the legend above] in 0.50 mM K_2CO_3 solutions.

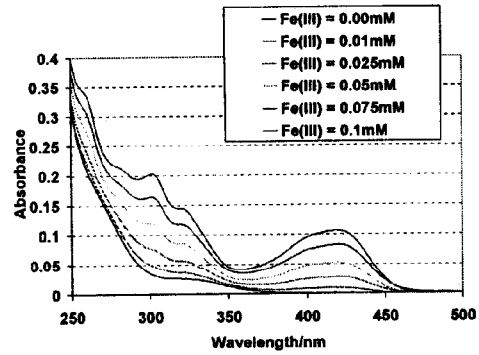

Fig. 3: UV Spectra for 0.075 mM $K_4Fe(CN)_6$ and a range of concentrations of $K_3Fe(CN)_6$ [denoted as Fe(III) in the legend above] in 0.75 mM K_2CO_3 solutions.

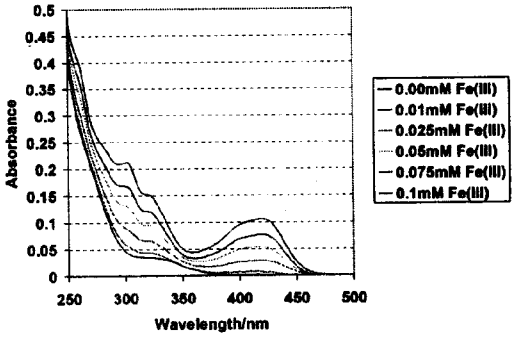

Fig. 4: UV Spectra for 0.100 mM $K_4Fe(CN)_6$ and a range of concentrations of $K_3Fe(CN)_6$ [denoted as Fe(III) in the legend above] in 1.00 mM K_2CO_3 solutions.

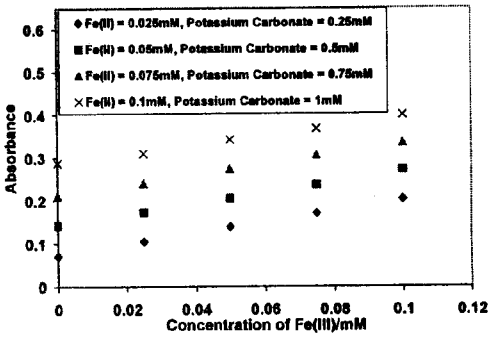

Fig. 5: Concentration of $K_3Fe(CN)_6$ [denoted as Fe(III) above while $K_4Fe(CN)_6$ is denoted as Fe(II)] against absorbance at 260 nm.

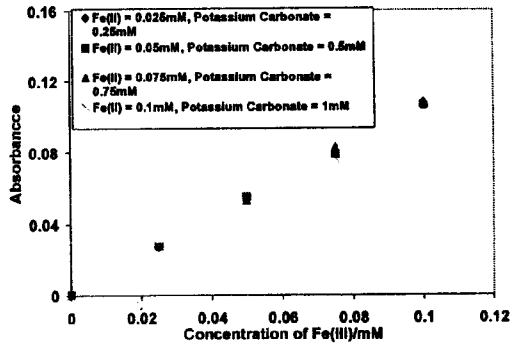

Fig. 6: Concentration of $K_3Fe(CN)_6$ [denoted as Fe(III) above while $K_4Fe(CN)_6$ is denoted as Fe(II)] against absorbance at 420 nm.

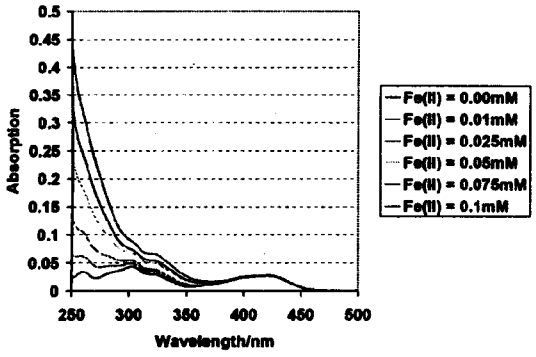

Fig. 7: UV spectra for 0.025 mM $K_3Fe(CN)_6$ and a range of concentrations of $K_4Fe(CN)_6$ [denoted as Fe(II) in the legend above] in 0.25 mM K_2CO_3 solutions.

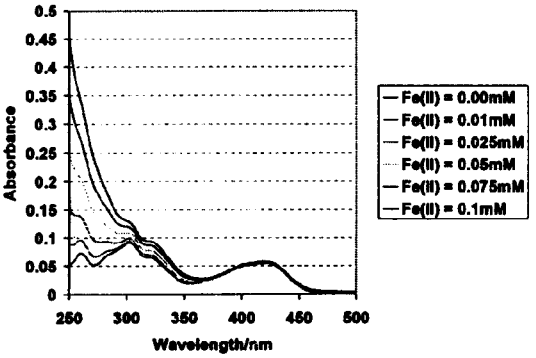

Fig. 8: UV spectra for 0.050 mM $K_3Fe(CN)_6$ and a range of concentrations of $K_4Fe(CN)_6$ [denoted as Fe(II) in the legend above] in 0.50 mM K_2CO_3 solutions.

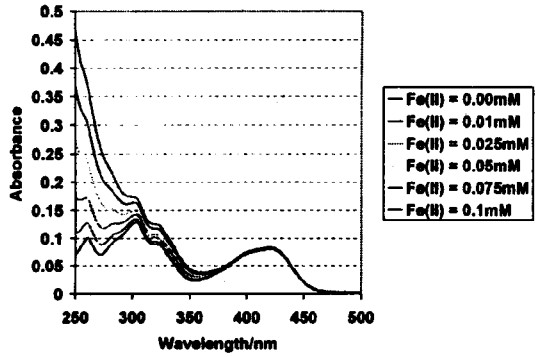

Fig. 9: UV spectra for 0.075 mM $K_3Fe(CN)_6$ and a range of concentrations of $K_4Fe(CN)_6$ [denoted as Fe(II) in the legend above] in 0.75 mM K_2CO_3 solutions.

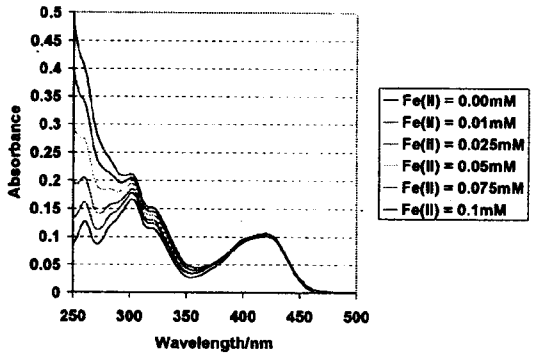

Fig. 10: UV spectra for 0.100 mM $K_3Fe(CN)_6$ and a range of concentrations of $K_4Fe(CN)_6$ [denoted as Fe(II) in the legend above] in 1.00 mM K_2CO_3 solutions.

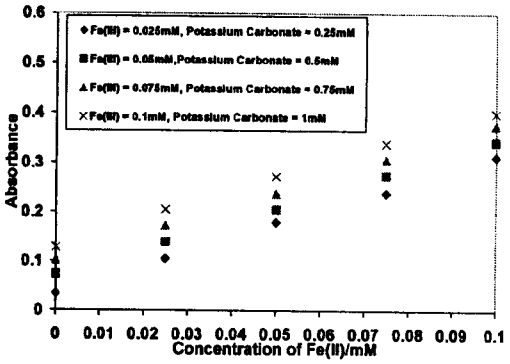

Fig. 11: Concentration of $K_4Fe(CN)_6$ [denoted as Fe(II) above while $K_3Fe(CN)_6$ is denoted as Fe(III)] against absorbance at 260 nm.

$K_3Fe(CN)_6$ was fixed and that of $K_4Fe(CN)_6$ was varied, the absorbance of UV light appeared to increase linearly with the concentration of $K_4Fe(CN)_6$ at wavelengths, λ = 323, 303 and 260 nm. This was confirmed by plotting absorbance at 260 nm with the concentrations of $K_4Fe(CN)_6$, as shown in Fig. 11, which gave a straight line as expected.

The absorbance of UV light by potassium carbonate was not found to interfere with those for ferro/ferricyanide ions [8]. Following Bae [8], absorbance at wavelengths of 420 and 260 nm were used for establishing correlations for the sample concentrations as given below.

If A_{420} and A_{260} refer to the absorbance at 420 and 260 nm respectively, while K_1, K_2, K_3 and K_4 refer to proportionality constants with C_1 and C_2 as

arbitrary constants, then linear relationships between the absorbance and concentration of ferro/ ferricyanide can be expressed as Equations 1 and 2. $[Fe(CN)_6^{3-}]$ and $[Fe(CN)_6^{4-}]$ are the concentrations of $Fe(CN)_6^{3-}$ (ferricyanide) and $Fe(CN)_6^{4-}$ (ferrocyanide) ions in the sample, respectively.

$$A_{420} = K_1[Fe(CN)_6^{3-}] + K_2[Fe(CN)_6^{4-}] + C_1 \quad (1)$$

$$A_{260} = K_3[Fe(CN)_6^{4-}] + K_4[Fe(CN)_6^{3-}] + C_2 \quad (2)$$

Fig. 5 and Fig. 6 were used for determining the relationship between absorbance of UV/Vis light and concentrations of $K_3Fe(CN)_6$ using a standard least squares fit of the data as explained below. Similarly Fig. 11 was used to determine a relationship between absorbance and concentrations of $K_4Fe(CN)_6$ using a standard least squares fit of data.

From plots of concentration against absorbance for standard samples at wavelengths of 420 and 260 nm and by using a least squares fit of the data, the values of K_1, K_2, K_3, K_4, C_1 and C_2 have been estimated as follows:

$K_1 = 1.058$; $K_2 = -0.003$; $K_3 = 1.260$

$K_4 = 2.724$; $C_1 = 0.000925$; $C_2 = 0.006421$

The correlations can now be written as shown in Equations 3 and 4:

$$A_{420} = 1.058[Fe(CN)_6^{3-}] - 0.003[Fe(CN)_6^{4-}] + 0.000925 \quad (3)$$

$$A_{260} = 1.260[Fe(CN)_6^{3-}] + 2.724[Fe(CN)_6^{4-}] + 0.006421 \quad (4)$$

The accuracy of these concentrations predicted from the above correlations was determined to be about ± 4% using standard solutions. Thus, it was verified that the correlations determined in this research are accurate enough for determining the concentrations of ferrocyanide and ferricyanide ions in any samples taken from the novel Redox Flow Battery described in the literature [1, 9-11].

Experimental

UV/Vis Spectroscopy was proposed as the analytical technique for determining the concentrations of potassium ferrocyanide $[K_4Fe(CN)_6]$ and potassium ferricyanide $[K_3Fe(CN)_6]$ ions in samples taken from the novel Redox Flow Battery described in the literature [1, 9-11]. A brief schematic representation of the flow reactor is shown in Fig. 12. As the colour of potassium ferrocyanide (Merck, Reagent grade) was pale yellow, it was anticipated that the solution would absorb within the ultraviolet (UV) region. The colour of potassium ferricyanide (Merck, Reagent grade) was bright yellow, indicating that it should absorb solely within the visible region. However, some interference was

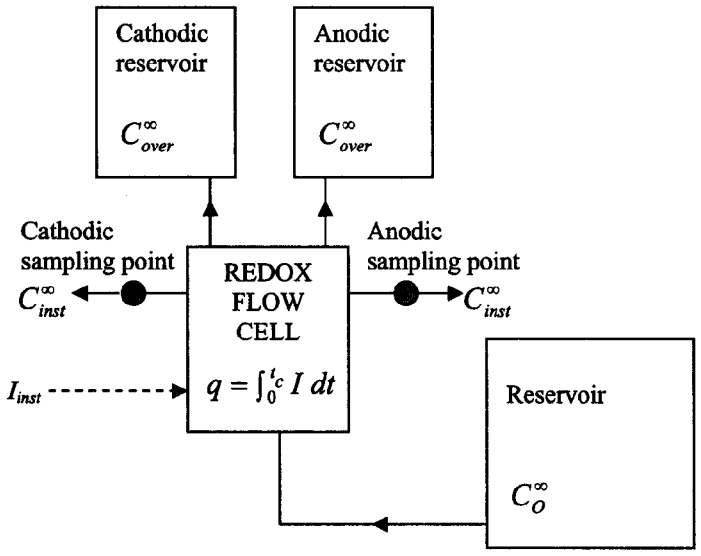

Fig. 12: Schematic diagram of the electrochemical separation of a mixture of $K_4Fe(CN)_6$ and $K_3Fe(CN)_6$.

observed by Bae [9] and thus experiments were designed in this research to investigate this. It was hypothesized that absorption in the UV region may have been due to the presence of functional groups or bond vibrations, but these were not detailed investigated during this work.

Experiments were conducted to determine the concentrations of $Fe(CN)_6^{4-}$ and $Fe(CN)_6^{3-}$ from a mixture in 0.5 M potassium carbonate (Merck, Reagent grade) using UV/Vis spectroscopy. Due to the possibility of interfering absorbance of UV and visible light by the two different ions, the mixtures were subjected to the lights of continuously changing wavelength while monitoring their absorbances. For this purpose, a range of standard solutions (0 to 0.1 mM ferrocyanide and 0 to 0.1 mM ferricyanide) were made up for determining the relationship between the absorbance of UV and visible light against the concentration of mixtures of $Fe(CN)_6^{4-}$ and $Fe(CN)_6^{3-}$ ions in aqueous solutions of K_2CO_3 as shown in Tables 1 and 2. In addition, the absorbance of 0.5 M K_2CO_3 was also determined.

Spectrometric analysis was conducted by means of a Perkin Elmer Lambda 10 UV/Vis spectrometer (double beam) in conjunction with a computer running UV Winlab software. Each scan was performed from 500 nm to 250 nm at a scan rate of 240 nm min^{-1}. The absorbance axis was adjusted to read from 0 to 1.5 arbitrary units [9].

In order to perform UV and visible scans on each sample, a quartz cell of dimensions 10 mm × 10 mm × 45 mm (Hellma) was employed. This was initially rinsed with de-ionised water before measuring the absorbance of the samples. A blank sample of de-ionised water was used to autozero the instrument before each set of measurements. The cell was emptied and filled with the sample and scanned between the aforementioned wavelength ranges. Once the scan was complete, the cell was emptied, rinsed and filled with the next sample for analysis.

Conclusions

UV/Vis spectroscopy was selected as the analytical tool for determining the concentrations of potassium ferrocyanide and potassium ferricyanide from experiments conducted on a novel Redox Flow Battery at the University of Manchester (cell design and operation has been described in detail in the literature [1, 9-11]). Suitable correlations were prepared to predict the concentrations from the absorbance spectra of the chemicals in both the visible and ultraviolet ranges. These correlations were tested against standard solutions and their accuracy was determined to be within ± 4%. As a result, an appropriate procedure was formulated using UV/Vis spectroscopy to determine the concentrations of potassium ferrocyanide and potassium ferricyanide from Redox Flow Battery samples accurately.

These correlations were used to evaluate the concentrations of potassium ferrocyanide and potassium ferricyanide in flow hydrodynamic experiments conducted on the novel Redox Flow Battery [1]. It was found from these hydrodynamic experiments that high reactant conversions (in excess of 90%) could be achieved for high concentrations of active redox species at low flow rates. UV-Vis spectroscopy thus proved to be an extremely useful tool in the characterization of the novel Redox Flow Battery as it has been for other types of electrochemical reactors [14-16].

Acknowledgements

Energy and Physical Sciences Research Council (EPSRC), UK for funding the research and University of Manchester for providing full laboratory facilities.

References

1. C. H. Bae, M. H. Chakrabarti and E. P. L. Roberts, *J. Appl. Electrochem.* **38**, 637 (2008).
2. M. Perrin, P. Malbranche, E. Lemaire-Potteau, B. Willer, M. L. Soria, A. Jossen, M. Dahlen, A. Ruddell, I. Cyphelly, G. Semrau, D. U. Sauer and G. Sarre, *J. Power Sources*, **154**, 545 (2006).
3. J. DeSilvestro, and O. Haas, *J. Electrochem. Soc.*, **137**, C5 (1990).
4. D. A. J. Rand, R. Woods and R. M. Dell, Batteries for Electric Vehicles, John Wiley & Sons Inc., New York (1998), p577.
5. C. Ponce de Le´on, A. Fr´ıas-Ferrer, J. Gonz´alez-Garc´ıa, D. A. Sz´anto and F. C. Walsh, *J. Power Sources*, **160**, 716 (2006).
6. M. Skyllas-Kazacos and F. Grossmith, *J. Electrochem. Soc.*, **134**, 2950 (1987).
7. P. Zhao, H. Zhang, H. Zhou and B. Yi, *Electrochim. Acta*, **51**, 1091 (2007).
8. B. Fang, Y. Wei, T. Arai, S. Iwasa and M. Kumagai, *J. Appl. Electrochem.*, **33**, 197 (2003).

9. Bae. C. H, Ph. D. Thesis. *Cell Design and Electrolytes of a Novel Redox Flow Battery* UMIST, Manchester, U.K., 2001.
10. B. K. Chakrabarti, Ph. D. Thesis, *Investigation of Electrolytes for a Novel Redox Flow Battery*, UMIST, Manchester, U.K., 2003.
11. M. H. Chakrabarti and E. P. L. Roberts, *NED Uni. J. Res.* **5**, 43 (2008).
12. T. Doherty, Ph. D. Thesis, *Mass Transfer Effects in Electrochemical Cells Containing Porous Electrodes*, UMIST, Manchester, U.K., 1996.
13. F. Coeuret, *J. Appl. Electrochem.*, **31**, 193 (2001).
14. W. M. Taama, R. E. Plimley and K. Scott, *Electrochim. Acta*, **41**, 549 (1996).
15. C. F. Oduoza, A. A. Wragg and M.A. Patrick, *Chem. Eng. J.*, **68**, 145 (1997).
16. T. Doherty, J. G. Sunderland, E. P. L. Roberts and D. J. Pickett, *Electrochim. Acta*, **41**, 519 (1996).
17. J. C. Gonza´lez-Jua´rez and J. Jime´nez-Becerril, *Rad. Phys. Chem.*, **75**, 768 (2006).
18. M. Darder, P. Aranda, M. Herna´ndez-Ve´lez, E. Manova and E. Ruiz-Hitzky, *Thin Solid Films*, **495**, 321 (2006).
19. A. M. Garcia Rodriguez, A. Garcia de Torres, J. M. Cano Pavon and C. Bosch Ojeda, *Talanta*, **47**, 463 (1998).
20. B. Roig, C. Gonzalez and O. Thomas, *Talanta*, **50**, 751 (1999).